Bicoherence Analysis for Condition Assessment of Multi-Faulted Helicopter Drivetrain Systems

Mohammed A. Hassan*, David Coats*, Yong-June Shin*, Abdel E. Bayoumi†, and Alexander Barry‡
*Department of Electrical Engineering, University of South Carolina, Columbia, SC, USA
†Department of Mechanical Engineering, University of South Carolina, Columbia, SC, USA
‡Contractor supporting US Army, VT Group, Redstone Arsenal, AL, USA

***Abstract*—Traditional linear spectral analysis techniques of the vibration signals, based on auto-power spectrum, are used as common tools of rotating components diagnoses. Unfortunately, linear spectral analysis techniques are of limited value when various spectral components interact with one another due to nonlinear or parametric process. In such a case, higher order spectral (HOS) techniques are recommended to accurately and completely characterize the vibration signals. In this paper, we use the bicoherence analysis as a tool to investigate nonlinear wave-wave interaction in vibration signals. Accelerometer data has been collected from an AH-64 helicopter drive-train research test bed simulating drive-train conditions under multiple faulted components namely faulted inner race in one hanger bearing, contaminated grease in another hanger bearing, misaligned and unbalanced drive shafts. The proposed bicoherence analysis provides more details about the spectral content of the vibration signal and how different fault frequencies nonlinearly interact with one another.**

I. Introduction

Condition Based Maintenance (CBM) (sometimes called Predictive Maintenance) is an approach where troubleshooting and repairing machines, or systems, are performed based continuous monitoring of their part's condition. Actions are taken through observation and analysis rather than on event of failure (Corrective Maintenance) or by following a strict maintenance time schedule (Preventive Maintenance). CBM program, if properly established and implemented, could significantly reduce the number or extent of maintenance operations, eliminate scheduled inspections, reduce false alarms, detect incipient faults, enable autonomic diagnostics, predict useful remaining life, enhance reliability, enable information management, enable autonomic logistics, and consequently reduced life cycle costs [1], [2].

Rotorcrafts form a unique subset of air vehicles in that its propulsion system is used not only for propulsion but also as the primary source of lift and maneuvering of the vehicle. Any failure in components of the propulsion or power transmission could lead to a complete loss of directional control and subsequent forced landing or crash [3]. The US Army and South Carolina Army National Guard (SCARNG) are currently employing the Vibration Management Enhancement Program (VMEP) [4] to shift the standard Time-Based Maintenance in military aviation toward the innovative CBM practice. Over the past decade, University of South Carolina (USC) has been working closely with SCARNG, U.S. Army Aviation Engineering Directorate (AED) and Intelligent Automation Corporation (IAC) on implementation of VMEP Program [5], [6]. These efforts expanded into a fully matured CBM Research Center within the USC Department of Mechanical Engineering, which hosts several aircraft component test stands in support of current US Army CBM objectives. Within the USC test facility is a complete AH-64 tail rotor drive train test stand TRDT, as shown in Figure 1. The test apparatus is used to collect data to be used in conjunction with historic helicopter vibration data to develop the baseline of operation for the systems under test. The signals being collected during the operational run of the apparatus included vibration data measured by the accelerometers, temperature measured via thermocouples, and speed and torque measurements. The measurement devices are placed at the forward and aft hanger bearings and both gearboxes as shown in Figure 1(a). Our aim is to improve the effectiveness of the CBM by developing new general methods for fault analysis that could be used in existing or new condition indicators.

Nevertheless, most of the conventional fault analysis techniques assume that a defect occurs in a rotating element separately, that we can identify this fault by the characterizing frequency of that component. For example, ball pass frequency inner-race rotating frequency (BPFI) is used to detect faults in the inner race of bearings [7]. However, it is not easy to detect this fault when it is combined with shaft faults, as will be discussed later in this paper. Due to interaction with the shaft fault, unexpected frequencies appear in the vibration spectrum which can not be explained by conventional power spectral analysis. In such cases, it would be helpful to analyze the vibration signals using higher order statistics (HOS), as will be introduced in the following section.

HOS analysis has been previously used in analyzing harmonic vibration interaction patterns for different combination of shaft misalignment and unbalance with good (healthy) hanger bearing [8]. In this paper, two different hanger bearing faults are analyzed under typically misaligned-unbalanced shafts. Experiment setup is described in sections III and results are then discussed in IV.

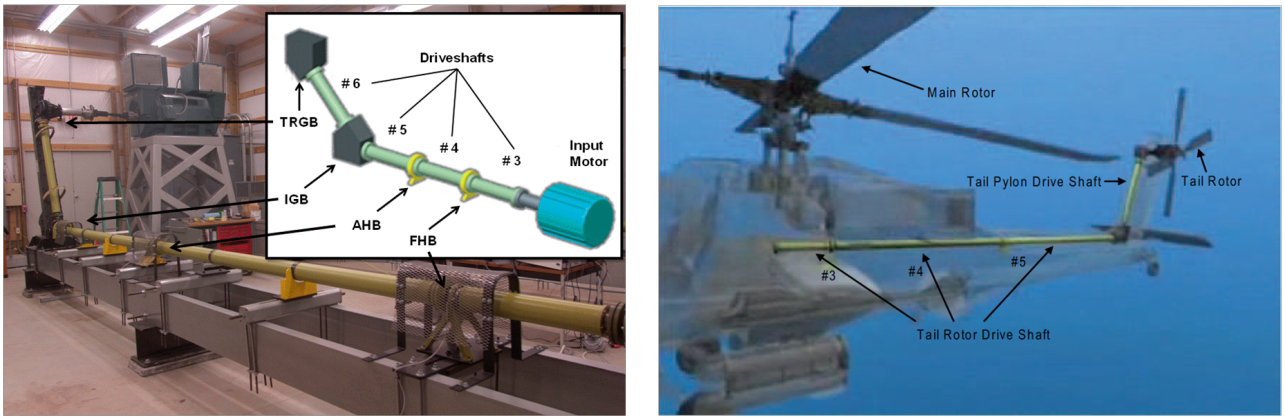

(a) (b)

Fig. 1. (a) TRDT test stand at USC and (b) Actual TRDT on AH-64

II. Bispectrum and Bicoherence

Vibration signals from mechanical systems are realizations of random process. Just as random variables are characterized by certain expected values or moments, random processes are characterized by their mean values, correlation function, and various higher order correlation functions. Alternatively, random processes may be characterized by the Fourier transforms of the various order correlation function [9]. For a stationary continuous vibration signal $x(t)$, the first order (linear) auto-correlation function $R_{xx}(\tau)$ and the power spectrum $S_{xx}(f)$ are Fourier transform pairs according to Wiener-Khinchin theorem [10], and can be estimated by (1) and (2).

$$R_{xx}(\tau) = E\{x^*(t)x(t+\tau)\} \tag{1}$$

$$S_{xx}(f) = E\{X^*(f)X(f)\} = E\{|X(f)|^2\} \tag{2}$$

The auto-power spectrum, $S_{xx}(f)$, has the dimensions of mean square values/Hz and it indicates how the mean square value is distributed over frequency. Auto-power spectrum is one of the most commonly used tools in spectrum analysis of vibration signals [11], [12].

Similarly, bispectrum $S_{xxx}(f_1, f_2)$ is the Fourier transform of the second-order correlation function $R_{xxx}(\tau_1, \tau_2)$, as given in (3) and (4), and it describes second-order statistical dependence between spectral components of signal $x(t)$.

$$R_{xxx}(\tau_1, \tau_2) = E\{x^*(t)x(t+\tau_1)x(t+\tau_2)\} \tag{3}$$

$$S_{xxx}(f_1, f_2) = E\{X(f_1)X(f_2)X^*(f_3 = f_1 + f_2)\} \tag{4}$$

The advantage of bispectrum over linear power spectral analysis is its ability to characterize quadratic nonlinearities in monitored systems [13], [14]. One of the characteristics of nonlinearities is that various frequencies "mix" to form new combinations of "sum" and "difference" frequencies, as depicted in Figure 2. An important signature is based on the fact that there exists a phase coherence, or phase coupling, between the primary interacting frequencies and the resultant new sum and difference frequencies [15]. Since all phase information is destroyed in computing the classical power spectrum, the power spectrum is incapable of detecting the phase coupling signature. The bispectrum describes this correlation between the three waves (source and the result of interaction process) in two-dimensional frequency space $(f_1 - f_2)$.

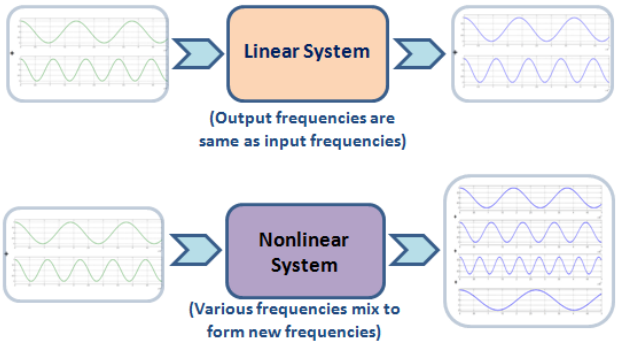

Fig. 2. Effect of nonlinear system on frequency mix (interaction) of input signals

The definition of the bispectrum in (4) shows how the bispectrum measures the statistical dependence between three waves. That is, $S_{xxx}(f_1, f_2)$ will be zero unless the following two conditions are met:

1. Waves must be present at the frequencies f_1, f_2, and f_1+f_2. That is, $X(f_1)$, $X(f_2)$, and $X(f_1 + f_2)$ must be non-zero.
2. A phase coherence must be present between the three frequencies f_1, f_2, and $f_1 + f_2$.

If waves present at f_1, f_2, and $f_1 + f_2$ are spontaneously excited independent waves, each wave will be characterized by statistical independent random phase. Thus, the sum phase of the three spectral components will be randomly distributed over $(-\pi, \pi)$. When a statistical averaging denoted by the expectation operator is carried out, the bispectrum will vanish due to the random phase mixing effect. On the other hand, if the three spectral components are nonlinearly coupled to each

other, the total phase of three waves will not be random at all, although phases of each wave are randomly changing for each realization. Consequently, the statistical averaging will not lead to a zero value of the bispectrum.

The magnitude of the bispectrum at coordinate point (f_1, f_2) measures the degree of phase coherence between the three frequency components f_1, f_2,and f_3. However, this magnitude is also dependent on the magnitude of the relevant Fourier coefficients. Therefore, a common function used to normalize the bispectrum is the bicoherence $b(f_1, f_2)$ [13].

$$b^2(f_1, f_2) = \frac{|S_{xxx}(f_1, f_2)|^2}{E\{|X(f_1)X(f_2)|^2\}E\{|X(f_3)|^2\}} : f_3 = f_1 + f_2 \quad (5)$$

The bicoherence is independent of the magnitude of the fourier transform and bounded by $0 \leq b_(f_1, f_2) \leq 1$, where 1 means complete coupling and 0 means no coupling at all.

III. Experimental set up and data description

The TRDT test stand, shown in Figure 1(a), is a full-scale AH-64 Helicopter tail rotor driveshaft apparatus for on-site data collection and analysis. The apparatus is a dynamometric configuration which includes an AC induction motor rated at 400hp controlled by variable frequency drive to provide input drive to the configuration, a multi-shaft drive train supported by hanger bearings, flex couplings at shaft joining points, two gearboxes, and an absorption motor of matching rating to simulate the torque loads that would be applied by the tail rotor blade. Vibration signals denoted as FHB and AHB, as shown in Figure 1, are collected from forward and aft hanger bearings at two minutes intervals at a sampling rate of 48 kHz.

Seeded hanger bearing faults testing was designed to include multi-faulted drive train components with two faulted hanger bearings running at the same time, one with a spalled inner race in the FHB position and one with contaminated grease with coarse grit sand run in the AHB position. This is done with 1.3° misalignment between drive shafts #3 and #4, 1.3° misalignment between drive shafts #4 and #5, and unbalanced drive shafts #3, #4 and #5 by 0.140 oz-in, 0.135 oz-in 0.190 oz-in respectively. The forward hanger bearing is machined to replicate a bearing with a spalled inner race as shown in Figure 3. All machining was done at the army research laboratory (ARL). The holes were milled into the inner race with a ball mill and were machined to the specs summarized in Table I.

TABLE I
Spalled Inner Race Information in the FHB position

Spall	Spall diameter (inch)	Spall depth (inch)	Distance from left shoulder (inch)	Distance from right shoulder (inch)
#1	0.030	0.017	0.1400	0.2538
#2	0.031	0.016	0.1956	0.1985
#3	0.031	0.017	0.2567	0.1376

The AHB has coarse grit contaminated grease mixed in a ratio of 5% by volume of the grease. This seeded fault is also done at the ARL with a representative sand contaminant consist of crushed quartz with the total particle size distribution as shown in Table II.

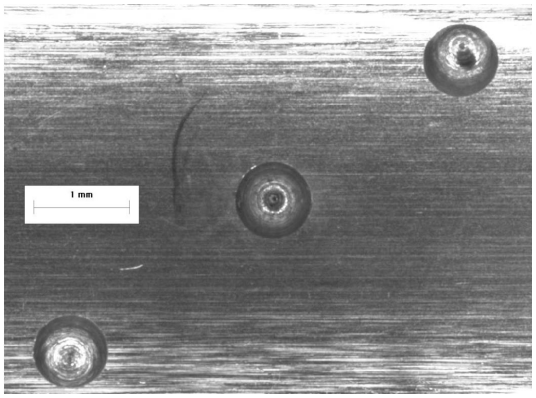

Fig. 3. Spalled Inner race seeded fault (FHB position)

TABLE II
Coarse Grit Contaminated Grease Mixture in the AHB position

Size (μ)	Volume fraction (%)
1	0.6 to 1.0
2	2.2 to 3.7
3	4.2 to 6.0
4	6.2 to 8.2
5	5.0 to 10.5
7	12.0 to 14.0
10	17.0 to 22.0
20	32.0 to 36.0
40	57.0 to 61.0
80	87.5 to 89.5
120	97.0 to 98.0
180	99.5 to 100
200	100

IV. Results and discussion

A. Spalled Inner Race Hanger Bearing

The power spectrum of the spalled inner race FHB is shown in Figure 4. It is estimated using average over ensemble of vibration data collected every two minutes over a 60 minutes run under output torque at the tail rotor equal to 111 lb-ft, and plotted with 1.465Hz frequency resolution. Due to the misaligned-unbalanced drive shafts, high magnitudes of the vibration exist at the 80.57Hz, 162.5Hz, and 243.2Hz as shown in Figure 4. These frequencies match 1SO , 2SO, and 3SO reported in Table III by the Aviation Engineering Directorate (AED). These shaft harmonics are typically used to describe shaft misalignment and unbalance by many vibration-analysis test-books [7], [16]. According to text books, one should also expect to see the ball pass inner-race frequency (BPFI) that characterizes the faulted hanger bearing under test, 441Hz as reported in Table III. However, it is not easy to detect the BPFI frequency in Figure 4. The highest non-shaft frequencies in this spectrum is at 684.1Hz and 279.8Hz which do not match any frequency in Table III. Therefore, it is obvious that linear spectral analysis fails to detect hanger bearing fault when it is combined with shaft faults, and also fails to relate all frequencies in the spectrum to known fault source.

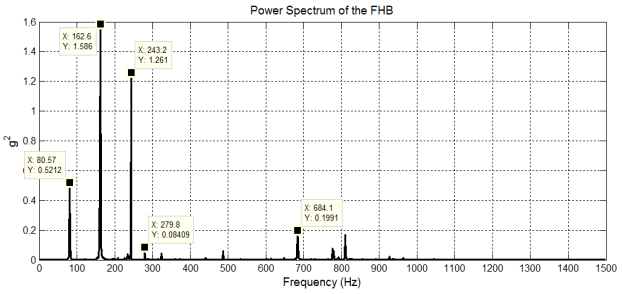

Fig. 4. Power spectrum of the spalled FHB with misaligned-unbalanced shafts

TABLE III
TRDT COMPONENTS ROTATING FREQUENCIES PROVIDED BY AED

Major Component	Source(s) or Meshing Components	Harmonic Number	Frequency Type	Frequency (Hz)	Frequency (RPM)
Tail Rotor Drive Shaft	Hanger Bearings	1	CFF	31.95	1917
	Hanger Bearings	2	CFF	63.90	3834
	Driveshaft	1	SO	81.06	4863
	Hanger Bearings	3	CFF	95.85	5751
	Hanger Bearings	4	CFF	127.80	7668
	Driveshaft	2	SO	162.11	9727
	Hanger Bearings	1	BSF	182.89	10974
	Driveshaft	3	SO	243.17	14590
	Hanger Bearings	1	BPFO	287.55	17253
	Driveshaft	4	SO	324.23	19454
	Hanger Bearings	2	BSF	365.79	21947
	Hanger Bearings	1	BPFI	441.96	26518
	Hanger Bearings	3	BSF	548.68	32921
	Hanger Bearings	2	BPFO	575.10	34506
	Hanger Bearings	4	BSF	731.57	43894
	Hanger Bearings	3	BPFO	862.65	51759
	Hanger Bearings	2	BPFI	883.92	53035
	Hanger Bearings	4	BPFO	1150.19	69012
	Hanger Bearings	3	BPFI	1325.89	79553
	Hanger Bearings	4	BPFI	1767.85	106071

The FHB vibration is then analyzed using bicoherence spectrum as shown in Figure 5. It can be seen that a number of shaft order harmonics exist along f_2= 80.57Hz, 161.1Hz, 243.2Hz. Along each of those frequencies in f_2 direction, there are number of quadratic coupling (nonlinear interaction) with other frequencies, in f_1 direction, including shaft harmonics and non-shaft frequencies. Shaft harmonic interaction patterns is used previously to assess drive shaft health conditions [8]. In our case here, we are concerned more about any interaction with *non-shaft* frequencies that might be related to hanger bearing faults.

For a better view, bicoherence spectrum is plotted by fixing f_2 to equal 161.1Hz and 243.2Hz and varying f_1 to investigate all frequencies interacting with those 2SO and 3SO including non-shaft frequencies. From Figure 6(b), bicoherence spectrum has a peak located at $b^2(f = 243.2\text{Hz}, f = 440.9\text{Hz}) = 0.4305$, which reflects interaction between the 3SO and the BPFI in Table III. The result of this interaction is a new frequency at the "sum" of the two coordinate frequencies which equal to 684.1Hz. This explains the presence of a spectral peak at this frequency in the power spectrum of the FHB vibration in Figure 4. From Figure 6(a), the value of $b^2(f = 161.1\text{Hz}, f = 279.8\text{Hz}) = 0.1669$ explains the source of 279.8Hz frequency in Figure 4. This bicoherence peak is due to interaction between SO2 and BPFI, but due to the the

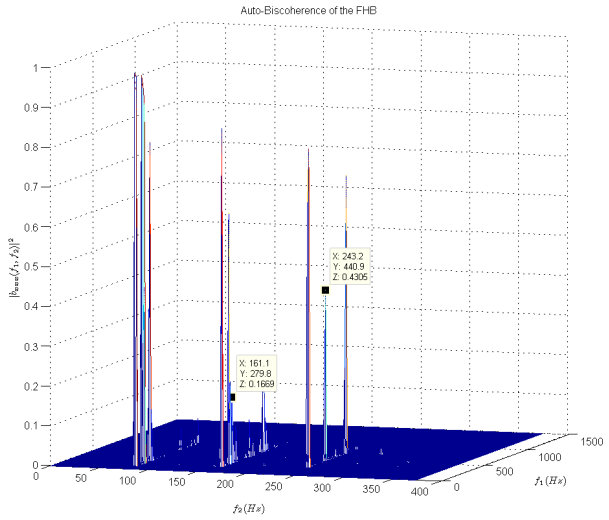

Fig. 5. Bicoherence of the FHB with misaligned-unbalanced shafts

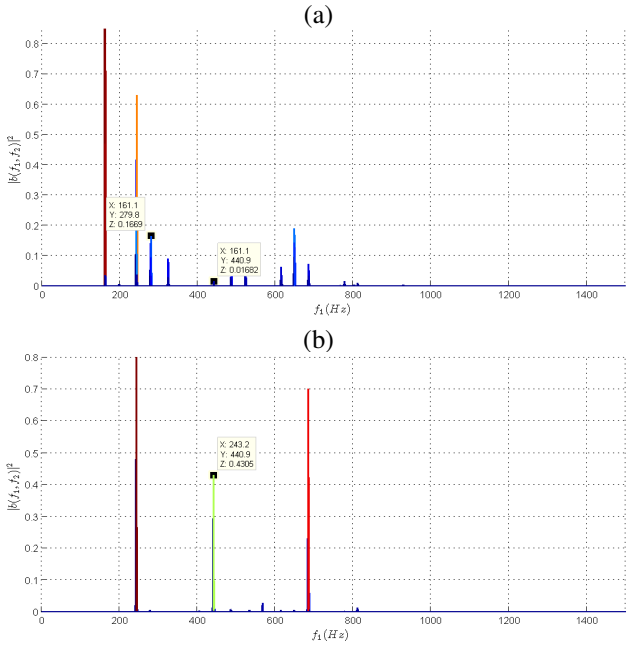

Fig. 6. Bicoherence of the FHB vibration showing frequency interactions with (a) $f_2 = 161.1$Hz, and (b) $f_2 = 243.2$Hz

way bicoherence is estimated in (4) and (5) it shows the least two frequencies (f_1 and f_2) in the three-wave coupled group (f_1, f_2, and $f_3 = f_1 + f_2$). Therefore, $b^2(f = 161.1\text{Hz}, f = 279.8\text{Hz})$ is indication of interaction between 2SO and the BPFI to create the "difference" frequency at 279.8Hz which appears in the power spectrum in Figure 4.

From the above discussion, it is clear that bicoherence spectrum is more useful in both detecting the hanger bearing fault and giving better explanation about source of frequencies in the vibration spectrum.

B. Coarse Grit Contaminated Grease Hanger Bearing

The power spectrum of the coarse grit contaminated grease AHB is shown in Figure 7. This fault does not have particular

frequency to characterize it in the power spectrum. Although it is clear from the vibration magnitudes that there is a fault in this bearing, the power spectrum still can not explain the source of generating high vibration magnitudes at 279.8Hz, 360.4Hz, 440.9Hz, 522.9Hz, 603.6Hz, 684.1Hz, 927.2Hz, and some other higher frequencies, which are spaced by the shaft rotating frequency 80.57Hz. The only frequency that can be related to TRDT frequencies in Table III is 440.9Hz, the BPFI of the faulted inner-race FHB.

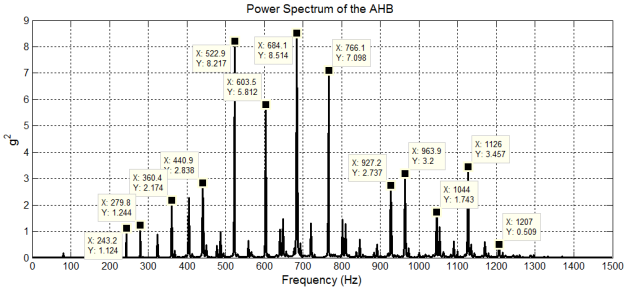

Fig. 7. Power spectrum of the coarse grit contaminated grease AHB

The bicoherence spectrum of the AHB vibration is shown in Figure 8 with vibration wave-wave interaction among a wide spread of shaft harmonics and non-harmonics frequencies. This indicates a very high nonlinear rotating medium that results in this large amount of interaction. Although it is hard to follow each coordinate point in the 3D bicoherence plot, we observe that there are particular frequencies over f_2 direction that interact with other frequencies, namely Shaft Orders 1SO, 2SO, 3SO, ...,8SO, and 279.8Hz, 360.4Hz, 440.9Hz, 522.9Hz, 603.6Hz, 684.1Hz. Again, for a better view, bicoherence spectrum is plotted along $f_2 = 80.75$Hz and 279.8Hz as shown in Figure 9. The trend of vibration interaction is clear that shaft harmonics tend to interact with the BPFI group that transferred from the FHB through drive shaft #4, with no other obvious source of interaction. The higher magnitude of the BPFI group of frequencies in the AHB spectrum in Figure 7 can be explain by multiple coordinate points of interaction in the bicoherence spectrum between shaft harmonics and frequencies generated at FHB. For example, 522.9Hz can be generated by frequency mix between the following coordinate pairs (279.8+3SO), (440.9+1SO), and (684.1-1SO).

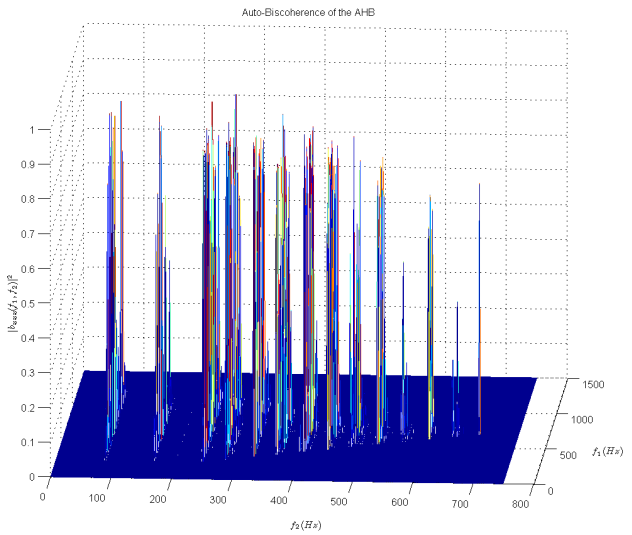

Fig. 8. Bicoherence the coarse grit contaminated grease AHB

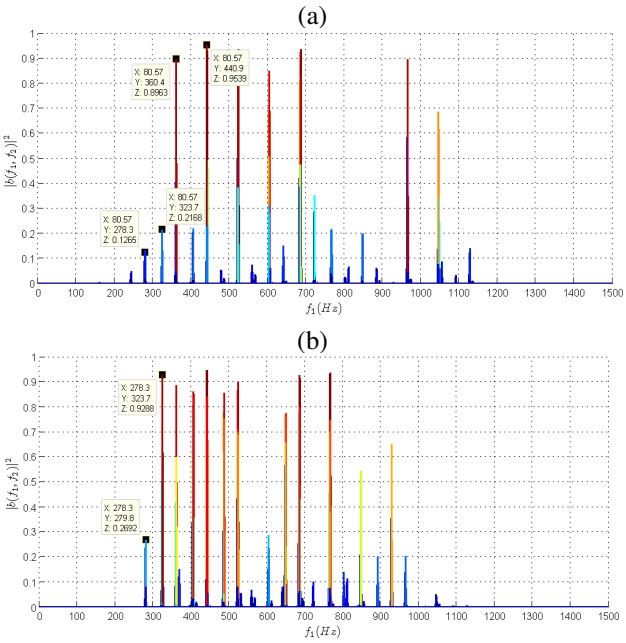

Fig. 9. Bicoherence of the AHB vibration showing interaction with (a) $f_2 = 80.57$Hz, and (b) $f_2 = 279.8$Hz

V. CONCLUSION

In this paper, bicoherence analysis has been used as a tool to investigate nonlinear wave-wave interaction in vibration signals from an AH-64 helicopter drive-train simulating accelerated drive-train conditions under multiple faulted components. TRDT has been tested typically with faulted inner race in one hanger bearing, contaminated grease in another hanger bearing, misaligned and unbalanced drive shafts. The proposed bicoherence analysis provided more details about the spectral content of the vibration signal and how different fault frequencies nonlinearly interact with one another. Compared to linear power spectrum, bicoherence enables us to both detect the hanger bearing faults and to explain the source of new generated frequencies appear in the power spectrum of the vibration signal. Studying these cases by use of bicoherence spectrum was useful to closing the loop between physical source of non-linearities and resultant frequencies showing up in the power spectrum of the vibration signal.

Since bicoherence showed better capability than linear power spectral analysis in studying this extreme case of multi-faults, future work would extend the study to include more faulted hanger bearing but with single shaft fault (misalignment or unbalance only). Since shaft faults are typical in many cases with the first three shaft harmonics dominating (1SO, 2SO, 3SO), focusing on vibration interaction with those particular frequencies in the bicoherence of hanger bearing is also recommended and can carry more useful information than the conventional power spectrum.

ACKNOWLEDGMENT

This research is funded by the South Carolina Army National Guard and United States Army Aviation and Missile Command via the Conditioned-Based Maintenance (CBM) Research Center at the University of South Carolina-Columbia. Also, this research is partially supported by the Egyptian government via the Government Mission Program for Mohammed Hassan, and National Science Foundation Faculty Early Career Development (CAREER) Program as well as a National Science Foundation Graduate Research Fellowship for David Coats.

REFERENCES

[1] A. Bayoumi, W. Ranson, L. Eisner, and L.E. Grant, "Cost and effectiveness analysis of the AH-64 and UH-60 on-board vibrations monitoring system," *IEEE Aerospace Conference,* pp. 3921-3940, Mar. 2005.

[2] V. Blechertas, A. Bayoumi, N. Goodman, R. Shah, and Yong-June Shin, "CBM Fundamental Research at the University of South Carolina: A Systematic Approach to U.S. Army Rotorcraft CBM and the Resulting Tangible Benefits," *Proceedings of AHS International Specialists' Meeting on Condition Based Maintenance,* Huntsville, AL, Feb. 2009.

[3] James J. Zakrajsek,et al. "Rotorcraft Health Management Issues and Challenges," *First International Forum on Integrated System Health Engineering and Management in Aerospace,* Napa, California, February 2006.

[4] P. Grabill, T. Brotherton, J. Berry, and L. Grant, "The US Army and National Guard Vibration Management Enhancement Program (VMEP): Data Analysis and Statistical Results," *American Helicopter Society 58th Annual Forum,* Montreal, Cananda, June, 2002.

[5] A. Bayoumi, and L. Eisner, "Transforming the US Army through the Implementation of Condition-Based Maintenance," *Journal of Army Aviation,* May 2007.

[6] A. Bayoumi, N. Goodman, R. Shah, L. Eisner, L. Grant, and J. Keller, "Conditioned-Based Maintenance at USC - Part I: Integration of Maintenance Management Systems and Health Monitoring Systems through Historical Data Investigation," *Proceedings of AHS International Specialists' Meeting on Condition Based Maintenance,* Huntsville, AL, Feb. 2008.

[7] R. K. Mobley, "Failure-Mode Analysis," in *An Introduction to predictive Mainenance,* Elsevier, 2002.

[8] M. A. Hassan, D. Coats, K. Gouda, Yong-June Shin, and A. Bayoumi, "Analysis of Nonliear Vibration-Interaction Using Higher Order spectra to diagnose aerospace system faults," *2012 IEEE Aerospace Conference*, March 2012.

[9] Boualem Boashash, Edward J. Powers, Abdelhak M. Zoubir, "*Higher-Order Statistical Signal Processing,*" Wiley, 1996.

[10] Leon W. Couch II, "*Digital and Analog Communications Systems (sixth ed.),* New Jersey, Prentice Hall, 2001, pp. 406409.

[11] A. S. Sait, and Y. I. Sharaf-Eldeen, "A Review of Gearbox Condition Monitoring Based on vibration Analysis Techniques Diagnostics and Prognostics," in *Rotating Machinery, Structural Health Monitoring, Shock and Vibration*, Vol. 8, T. Proulx, Ed. New York: Springer, 2011, pp. 307-324.

[12] P. D. Samuel, and D. J. Pines, "A review of vibration-based techniques for helicopter transmission diagnostics," *Journal of Sound and Vibration*, vol. 282, no. 1-2, pp. 475-508, Apr. 2005.

[13] Y. C. Kim, and E. J. Powers, "Digital bispectral analysis and its application to nonlinear wave interactions," *IEEE Transactions on Plasma Science*, vol. 7, no. 2, pp. 120-131, July 1979.

[14] S. Elgar, and R.T. Guza, "Statistics of bicoherence," *IEEE transaction on Acoustics Speech and Signal Processing*, vol. 36, no. 10, pp. 1667-1668, Oct. 1988.

[15] T. Kim, W. Cho, E. J. Powers, W. M. Grady, and A. Arapostathis, "ASD system condition monitoring using cross bicoherence," *2007 IEEE electricship technologies symposium*, pp. 378-383, May 2007.

[16] C. Scheffer, P. Girdhar, "*Practical Machinery Vibration Analysis and Predictive Maintenance,*" 2004.